

Probing the fractional topological charge of a vortex light beam by using dynamic angular double slits

Jing Zhu,¹ Pei Zhang,^{1,2,*} Dongzhi Fu,¹ Dongxu Chen,¹ Ruifeng Liu,¹ Yingnan Zhou,¹
Hong Gao,¹ and Fuli Li¹

¹Laboratory of Quantum Information and Quantum Optoelectronic Devices, Shaanxi Province,
Xian Jiaotong University, Xian 710049, China

²Key Laboratory of Quantum Information, University of Science and Technology of China,
Chinese Academy of Science, Hefei 230026, China

*Corresponding author: zhangpei@mail.ustc.edu.cn

Received June 28, 2016; revised August 6, 2016; accepted August 6, 2016;
posted August 9, 2016 (Doc. ID 269178); published September 8, 2016

Vortex beams with fractional topological charge (FTC) have many special characteristics and novel applications. However, one of the obstacles for their application is the difficulty of precisely determining the FTC of fractional vortex beams. We find that when a vortex beam with an FTC illuminates a dynamic angular double slit (ADS), the far-field interference patterns that include the information of the FTC of the beam at the angular bisector direction of the ADS vary periodically. Based on this property, a simple dynamic ADS device and data fitting method can be used to precisely measure the FTC of a vortex light beam with an error of less than 5%. © 2016 Chinese Laser Press

OCIS codes: (050.4865) Optical vortices; (120.3180) Interferometry; (140.3295) Laser beam characterization.
<http://dx.doi.org/10.1364/PRJ.4.000187>

Since Allen *et al.* recognized in 1992 that vortex optical fields with a phase distribution of the form $\exp(im\phi)$ [ϕ is the azimuthal angle and m is the azimuthal index referring to the topological charge (TC) of the optical vortex] may carry orbital angular momentum (OAM) [1], vortex light beams have been extensively studied both theoretically and experimentally. Traditionally, m is an integer, such as Laguerre–Gaussian laser modes. Then the optical field is called an integral vortex optical field, which is an eigenstate of the OAM operator with eigenvalue of $m\hbar$, and has an annular intensity distribution with a dark central node produced by the central phase singularity [1,2]. Integral vortex light beams have offered a good source both in classical and quantum optics with many different applications [3], such as optical tweezers and micromanipulation [4–8], optical communications [9–11], quantum information science [12–15], spiral phase contrast imaging [16], and holographic ghost imaging [17].

On the other hand, the situation becomes more complex and interesting when the TC is an arbitrary fractional number. Since Berry introduced the characteristics and the evolving of fractional vortex beams mathematically in 2004 [18], fractional vortex beams have attracted increasing attention. A fractional vortex beam has a phase distribution of the form $\exp[i(M\phi + \beta)]$ somewhere during its propagation, where M is an arbitrary fractional number and β is the angular position of the helical wavefront cut (angular phase discontinuity). Due to the radial phase discontinuity in fractional vortex optical fields, the axis symmetry of intensity found in integer-order optical vortices is broken and a low-intensity radial strip has been observed [18,19]. Meanwhile, the state, instead of the eigenstate of OAM in integer vortex optical fields, is a superposition state of the basis of integer OAM states that

depend on both the TC M and angular position β [20–22]. The characteristics of the fractional vortex optical fields endow them with unique advantages compared to the integer vortex optical fields. For example, as a fractional vortex beam has a radial opening, this could be used to guide and transport particles [23] and improve the ability of optical sorting [24]. The asymmetric intensity distribution also could be utilized to achieve anisotropic edge enhancement [25,26]. In quantum information processing, it could be used to investigate high-dimensional entanglement states by utilizing non-integer OAMs [20,27,28]. One of the key issues for the above applications is the effective determination of the fractional TC (FTC). Many methods that have been used for integral TC determination by calculating the number of interference patterns, such as dual-triangular aperture diffraction [29], triangular aperture diffraction [30], mode conversion [31], and interference with its mirror image [32], could be used to observe only the half-integer value of a fractional vortex beam but not for probing the exact value of an FTC. Nevertheless, there are still several methods to measure the FTC. Liu put forward a potential way based on a weak random scattering screen by counting the size of the area of divided bright spots for the fractional parts of the TC and the number of the complete spots for the integral parts [33]. Zhang probed the FTC using a vortex grating spectrum analyzer within a 10% error [34]. During their experiments the intensity value of the center portion of the target diffraction order was extracted to calculate the FTCs, and the target diffraction order was N or $N + 1$, where $N \leq -M \leq N + 1$. This means the range of the FTC must be known beforehand. Huang *et al.* designed a method of cascaded Mach–Zehnder interferometers (MZIs) to measure the FTC of a light beam [35]. This method needs more

than three cascaded MZIs when the modulus of the FTC is larger than 2. The larger the modulus of the FTC, the more cascading stages are needed. That is to say, the stability and the precision will decrease for larger FTC. Li *et al.* proposed a method to identify nondestructively the vortex light by using modified MZIs [36]. The key point of this method is the relationship between the intensity difference of two outputs in the setup; the modified MZIs method also needs precise control of the relative phase change when the modulus of the FTC become larger. The larger the modulus of the FTC, the more difficult is the experiment. Meanwhile, important disadvantages for MZIs are that they are phase sensitive and unstable. Emile *et al.* determined the FTC by a Fresnel bi-prism with error of less than 6% [37]. This method calls for precisely aligning the angular phase discontinuity with the top of the prism and precisely identifying the center of the interference fringes. Most of the methods described here need a complicated experimental setup or have lower precision.

Based on previous work reported in Refs. [38–40], a simple setup with a dynamic angular double slit (ADS) can be employed to precisely measure the FTC of vortex beams.

According to our previous work [40], when a vortex beam with a spiral phase front $\exp(il\phi)$ passes through a dynamic ADS along the z' axis, as shown in Fig. 1, the interference pattern intensity at P varies as a cosine function of $l\varphi$, $I \propto 1 + \cos(l\varphi + \theta)$, where φ is the angle between the dynamic ADS, and θ is an additional phase set on one slit. This method also works well for a fractional vortex beam with the spiral phase front $\exp[i(M\phi + \beta)]$. The result is

$$I \propto 1 + \cos[M(\varphi + \theta/M)]. \quad (1)$$

As shown in Fig. 1, the angular bisector direction of the dynamic ADS is parallel to the y axis and the y' axis. We can then fix the angular bisector at the y axis and continuously rotate the two single slits with the same angular velocity with respect to the y axis. Thus, a periodic bright or dark intensity can be obtained at the y' axis when a vortex beam illuminates the ADS. After the intensity is collected at P , the $I - \varphi$ curve can be gotten. When one of the slits moves to the position of a helical wavefront cut, there will be a sharp change in the $I - \varphi$ curve, which could help us to determine β .

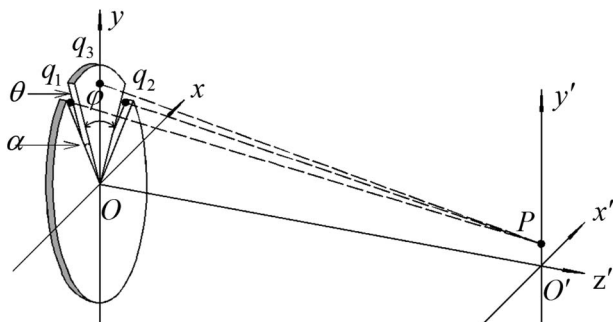


Fig. 1. Schematic of ADS interference. α is the width of an angular single slit, and φ is the angle between dynamic two single slits. q_1 , q_2 , and q_3 are three points on the mask and oq_3 is the angular bisector of $\angle q_1oq_2$. P is a point on the far field (with $q_1P = q_2P$), which is chosen to observe interferential intensity. θ represents an additional phase on one single slit.

After the experimental data about I with φ has been obtained, it is reasonable to get the FTC by fitting those data. Because any function that has the expression of $a \sin(x) + b \cos(x)$ can be simplified to $\sqrt{a^2 + b^2} \cos(x - \gamma)$, where $\sin(\gamma) = a/\sqrt{a^2 + b^2}$, we choose the fitting function as

$$I_0 = a_0 + a_1 \sin(M_t\varphi) + b_1 \cos(M_t\varphi). \quad (2)$$

To minimize the fitting error, none of the parameters in Eq. (2) can be fixed. If $\theta = 0$, we can get only the modulus of the FTC. To determine the sign of the FTC, the additional phase θ must be introduced [40]. First, we collect the intensity when the additional phase θ is zero. Second, we record the intensity again when θ is set to be $\pi/2$. Finally, we can get the sign of the FTC from the direction of displacement of the intensity period (or a rotation in polar coordinates of the $I - \varphi$ curves) between the two curves. It can be known from Eq. (1) that, if θ is positive, the second curve will rotate clockwise when the sign of M is positive and anticlockwise while the sign of M is negative. Based on these methods, we propose a simple, quick, and accurate method for measuring the modulus and sign of the FTC simultaneously.

The experimental setup of the ADS interference is shown in Fig. 2. Light from an He-Ne laser passes through a half-wave plate (HWP) and a polarizing beam splitter (PBS), which are used to adjust intensity and filter the polarization. Then it is expanded by two lenses, L1 and L2. The expanded beam is vertically illuminated on a spatial light modulator (SLM), which is used to generate vortex beams and ADSs. The far-field diffraction is generated by lens L3 and the first-order diffraction is selected by an aperture. Finally, the intensity pattern is recorded by a charge-coupled device (CCD) camera. For simplicity, we fix both the angular bisector of the ADS and the position of helical phase cut on the y axis, which means the direction angle of the angular bisector and β are both zero, so the center of interference patterns will not move when the angle of the ADS is changed. By integrating the intensity in the center, we can obtain the experimental data about the $I - \varphi$ relationship. In the experimental process, the width of an angular single slit is 8° , the step of two-slit rotation is 1° , and the resolution of the SLM is $20 \mu\text{m}$ per pixel.

Figure 3 shows the experimental result for determining the modulus of the FTC of different vortex beams with additional phase $\theta = 0$. The black dots are the experimental data, while the green curves are their fitting results. M is the FTC we generated and M_f is the probing result from our method. The errors between M and M_f are all less than 5% in our experiment ($M = \pm 1.5, \pm 4.3, \pm 7.8, \pm 15.2$ are chosen). Thus, our method

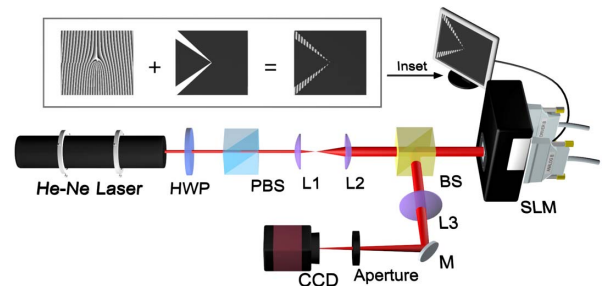


Fig. 2. Sketch of the experimental setup. The inset shows the mask pattern loaded on the SLM.

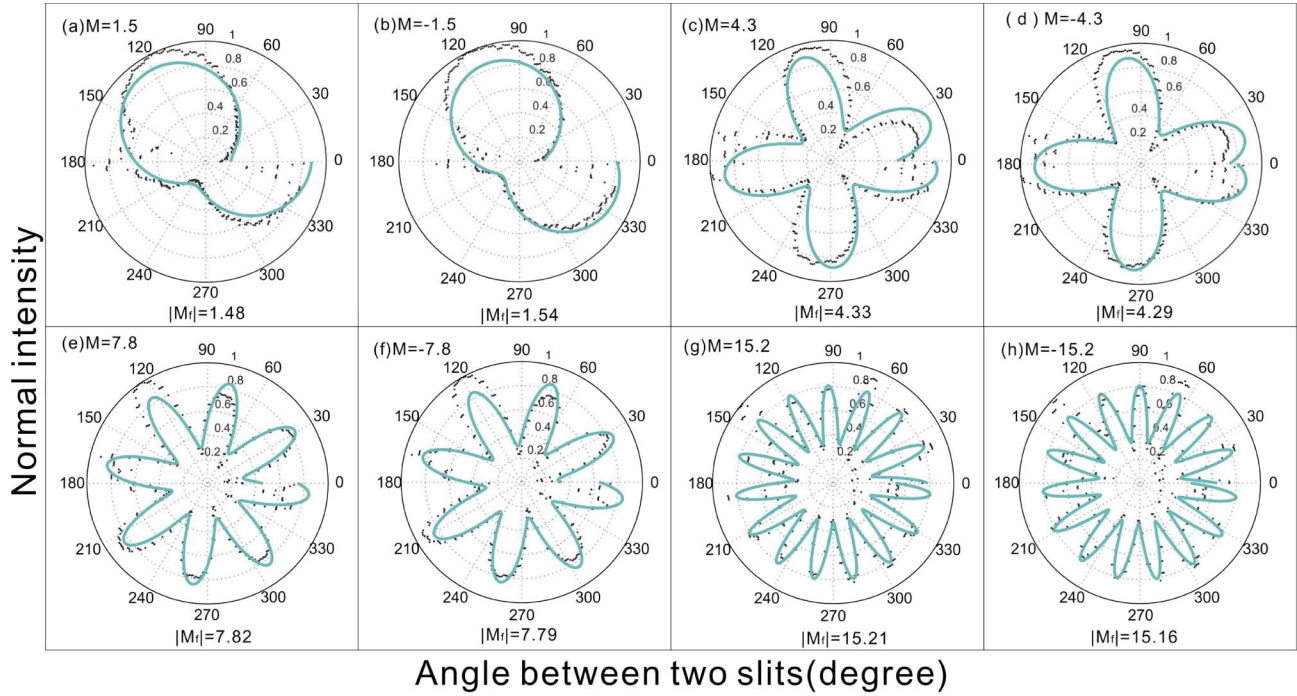


Fig. 3. $I - \varphi$ curves in polar coordinates when the additional phase θ is zero. The black dots are the experimental data and the green solid curves are fits of the data. M is the theoretical FTC and $|M_f|$ is the modulus of the FTC, which is obtained by fitting the experimental data to the fitting function.

is both precise and suitable for wide ranges. According to Eq. (1), the minimum value of the data is zero. The experimental data in Fig. 3 are not consistent with the theory. This is because of the existence of background light. However, this will not change the period of the curve. That is, the modulus of M will not be affected.

In Fig. 4, the purple curve, which has the additional phase $\pi/2$, rotates 21° clockwise compared with the blue one, in which the additional phase is zero. From Eq. (1), we know that when the additional phase difference between two measurements is $\Delta\theta = \theta_2 - \theta_1$, the rotation angle will be $\Delta\theta/M$. The experimental result is consistent with the theoretical value, which is 20.93° .

The errors come mainly from the width of angular single slit α , the rotating step of the two slits $\Delta\varphi$, and nonideal

instruments used in the experiment. The width of an angular single slit cannot be too wide, because more helical phase will be selected by the slits, which will affect the interference pattern. It also cannot be too small, because less intensity will be collected by the detector. The rotating step of the two slits $\Delta\varphi$ should be small enough to get more experimental data, especially for a high-order FTC beam.

In conclusion, we have shown that dynamic ADS can be used to measure the FTC of a vortex light beam easily and precisely. When an FTC vortex beam illuminates the ADS, the far-field interference patterns at the angular bisector direction of the ADS vary periodically, which include the information of the FTC. Based on this, the modulus of the FTC can be easily probed by fitting the experimental data with the error of less than 5%. The sign of the FTC can be judged by adding an additional phase θ on one of the slits. This method clearly reveals the spiral phase structure of FTC vortex beams, and provides a way to precisely measure FTCs with a very simple and low-cost structure.

Funding. Fundamental Research Funds for the Central Universities; National Natural Science Foundation of China (NSFC) (11374008, 11374238, 11374239, 11534008).

REFERENCES

1. L. Allen, M. W. Beijersbergen, R. J. C. Spreeuw, and J. P. Woerdman, "Orbital angular momentum of light and the transformation of Laguerre-Gaussian laser modes," *Phys. Rev. A* **45**, 8185–8189 (1992).
2. S. J. van Enk and G. Nienhuis, "Eigenfunction description of laser beams and orbital angular momentum of light," *Opt. Commun.* **94**, 147–158 (1992).
3. S. Franke-Arnold, L. Allen, and M. Padgett, "Advances in optical angular momentum," *Laser Photon. Rev.* **2**, 299–313 (2008).

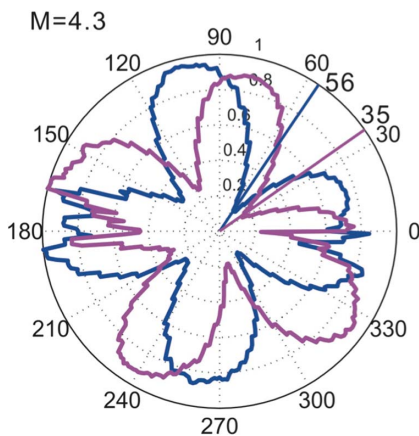


Fig. 4. Contrasted $I - \varphi$ curves between $\theta = 0$ (the blue curve) and $\theta = \pi/2$ (the purple curve) with $M = 4.3$.

4. K. Dholakia and T. Čížmár, "Shaping the future of manipulation," *Nat. Photonics* **5**, 335–342 (2011).
5. H. He, M. E. J. Friese, N. R. Heckenberg, and H. Rubinsztein-Dunlop, "Direct observation of transfer of angular momentum to absorptive particles from a laser beam with a phase singularity," *Phys. Rev. Lett.* **75**, 826–829 (1995).
6. N. B. Simpson, K. Dholakia, L. Allen, and M. J. Padgett, "Mechanical equivalence of spin and orbital angular momentum of light: an optical spanner," *Opt. Lett.* **22**, 52–54 (1997).
7. M. J. Padgett and R. Bowman, "Tweezers with a twist," *Nat. Photonics* **5**, 343–348 (2011).
8. D. G. Grier, "A revolution in optical manipulation," *Nature* **424**, 810–816 (2003).
9. G. Gibson, J. Courtial, and M. J. Padgett, "Free-space information transfer using light beams carrying orbital angular momentum," *Opt. Express* **12**, 5448–5456 (2004).
10. J. Wang, J.-Y. Yang, I. M. Fazal, N. Ahmed, Y. Yan, H. Huang, Y. Ren, Y. Yue, S. Dolinar, M. Tur, and A. E. Willner, "Terabit free-space data transmission employing orbital angular momentum multiplexing," *Nat. Photonics* **6**, 488–496 (2012).
11. N. Bozinovic, Y. Yue, Y. Ren, M. Tur, P. Kristensen, H. Huang, A. E. Willner, and S. Ramachandran, "Terabit-scale orbital angular momentum mode division multiplexing in fibers," *Science* **340**, 1545–1548 (2013).
12. A. Mair, A. Vaziri, G. Weihs, and A. Zeilinger, "Entanglement of the orbital angular momentum states of photons," *Nature* **412**, 313–316 (2001).
13. G. Molina-Terriza, J. P. Torres, and L. Torner, "Management of the angular momentum of light: preparation of photons in multi-dimensional vector states of angular momentum," *Phys. Rev. Lett.* **88**, 013601 (2001).
14. J. Leach, B. Jack, J. Romero, A. K. Jha, A. M. Yao, S. Franke-Arnold, D. G. Ireland, R. W. Boyd, S. M. Barnett, and M. J. Padgett, "Quantum correlations in optical angle-orbital angular momentum variables," *Science* **329**, 662–665 (2010).
15. J. E. Curtis and D. G. Grier, "Structure of optical vortices," *Phys. Rev. Lett.* **90**, 133901 (2003).
16. S. Fürhapter, A. Jesacher, S. Bernet, and M. Ritsch-Marte, "Spiral phase contrast imaging in microscopy," *Opt. Express* **13**, 689–694 (2005).
17. B. Jack, J. Leach, J. Romero, S. Franke-Arnold, M. Ritsch-Marte, S. M. Barnett, and M. J. Padgett, "Holographic ghost imaging and the violation of a bell inequality," *Phys. Rev. Lett.* **103**, 083602 (2009).
18. M. V. Berry, "Optical vortices evolving from helicoidal integer and fractional phase steps," *J. Opt. A* **6**, 259–268 (2004).
19. J. Leach, E. Yao, and M. J. Padgett, "Observation of the vortex structure of a non-integer vortex beam," *New J. Phys.* **6**, 71 (2004).
20. S. S. R. Oemrawsingh, A. Aiello, E. R. Eliel, G. Nienhaus, and J. P. Woerdman, "How to observe high-dimensional two-photon entanglement with only two detectors," *Phys. Rev. Lett.* **92**, 217901 (2004).
21. A. Aiello, S. S. R. Oemrawsingh, E. R. Eliel, and J. P. Woerdman, "Nonlocality of high-dimensional two-photon orbital angular momentum states," *Phys. Rev. A* **72**, 052114 (2005).
22. J. B. Götte, K. O'Holleran, D. Preece, F. Flossmann, S. Franke-Arnold, S. M. Barnett, and M. J. Padgett, "Light beams with fractional orbital angular momentum and their vortex structure," *Opt. Express* **16**, 993–1006 (2008).
23. S. Tao, J. Lin, and X. Peng, "Fractional optical vortex beam induced rotation of particles," *Opt. Express* **13**, 7726–7731 (2005).
24. C.-S. Guo, Y.-N. Yu, and Z. Hong, "Optical sorting using an array of optical vortices with fractional topological charge," *Opt. Commun.* **283**, 1889–1893 (2010).
25. G. Situ, G. Pedrini, and W. Osten, "Spiral phase filtering and orientation-selective edge detection/enhancement," *J. Opt. Soc. Am. A* **26**, 1788–1797 (2009).
26. G. Situ, M. Warber, G. Pedrini, and W. Osten, "Phase contrast enhancement in microscopy using spiral phase filtering," *Opt. Commun.* **283**, 1273–1277 (2010).
27. S. S. R. Oemrawsingh, J. A. de Jong, X. Ma, A. Aiello, E. R. Eliel, G. W. 't Hooft, and J. P. Woerdman, "High-dimensional mode analyzers for spatial quantum entanglement," *Phys. Rev. A* **73**, 032339 (2006).
28. G. F. Calvo, A. Picón, and A. Bramon, "Measuring two-photon orbital angular momentum entanglement," *Phys. Rev. A* **75**, 012319 (2007).
29. X. Li, Y. Tai, Z. Nie, H. Wang, H. Li, J. Wang, J. Tang, and Y. Wang, "Fraunhofer diffraction of Laguerre-Gaussian beam caused by a dynamic superposed dual-triangular aperture," *Opt. Eng.* **54**, 123113 (2015).
30. A. Mourka, J. Baumgartl, C. Shanor, K. Dholakia, and E. M. Wright, "Visualization of the birth of an optical vortex using diffraction from a triangular aperture," *Opt. Express* **19**, 5760–5771 (2011).
31. J. Zhou, W. Zhang, and L. Chen, "Experimental detection of high-order or fractional orbital angular momentum of light based on a robust mode converter," *Appl. Phys. Lett.* **108**, 111108 (2016).
32. W. M. Lee, X.-C. Yuan, and K. Dholakia, "Experimental observation of optical vortex evolution in a Gaussian beam with an embedded fractional phase step," *Opt. Commun.* **239**, 129–135 (2004).
33. M. Liu, "Probing the vortex beams with fractional and integral topological charges using weak random scattering screen," *Eur. Phys. J. D* **67**, 244 (2013).
34. N. Zhang, "Analysis of fractional vortex beams using a vortex grating spectrum analyzer," *Appl. Opt.* **49**, 2456–2462 (2010).
35. H.-C. Huang, Y.-T. Lin, and M.-F. Shih, "Measuring the fractional orbital angular momentum of a vortex light beam by cascaded Mach-Zehnder interferometers," *Opt. Commun.* **285**, 383–388 (2012).
36. P. Li, B. Wang, X. Song, and X. Zhang, "Non-destructive identification of twisted light," *Opt. Lett.* **41**, 1574–1577 (2016).
37. O. Emile, J. Emile, and C. Brousseau, "Determination of the topological charge of a twisted beam with a Fresnel bi-prism," *J. Opt.* **16**, 125703 (2014).
38. R. Liu, J. Long, F. Wang, Y. Wang, P. Zhang, H. Hao, and F. Li, "Characterizing the phase profile of a vortex beam with angular-double-slit interference," *J. Opt.* **15**, 125712 (2013).
39. H. Zhou, L. Shi, X. Zhang, and J. Dong, "Dynamic interferometry measurement of orbital angular momentum of light," *Opt. Lett.* **39**, 6058–6061 (2014).
40. D. Fu, D. Chen, R. Liu, Y. Wang, H. Gao, F. Li, and P. Zhang, "Probing the topological charge of a vortex beam with dynamic angular double slits," *Opt. Lett.* **40**, 788–791 (2015).